# Predicting the Future Land Use and Land Cover Changes for Bhavani Basin, Tamil Nadu, India Using QGIS MOLUSCE Plugin

**manikandan kamaraj** ( mk6714@srmist.edu.in )
SRM Institute of Science and Technology
**Sathyanathan Rangarajan**
SRM Institute of Science and Technology

**Research Article**

**Keywords:** Land use and Land cover, ANN-Multi layer perception, Predicted LULC, Bhavani basin, MOLUSCE, QGIS

**Posted Date:** July 8th, 2021

**DOI:** https://doi.org/10.21203/rs.3.rs-616393/v1



**Version of Record:** A version of this preprint was published at Environmental Science and Pollution Research on February 3rd, 2022. See the published version at https://doi.org/10.1007/s11356-021-17904-6.

# Predicting the Future Land Use and Land Cover Changes for Bhavani basin, Tamil Nadu, India Using QGIS MOLUSCE Plugin

**Manikandan Kamaraj**[1]
**Sathyanathan Rangarajan**[2]

**Abstract**

Human population growth, movement, and demand have a substantial impact on land use and land cover dynamics. Thematic maps of land use and land cover (LULC) serve as a reference for scrutinizing, source administration, and forecasting, making it easier to establish plans that balance preservation, competing uses, and growth compressions. The objective of this study is to identify the changeover of land-use changes in the Bhavani basin for the two periods 2005 and 2015, as well as to forecast and establish potential land-use changes in the year 2025 and 2030 by using QGIS 2.18.24 version MOLUSCE plugin (ANN-Multi layer perception) model. The five criteria, such as DEM, gradient, aspect, distance from the road and river, and built-up density, are used as spatial variable maps in the processes of learning in ANN-Multi layer perception to predict their influences on LULC between 2005 and 2010 and it was found that DEM, distance from the road and river, and built-up density have significant effects. The projected and accurate LULC maps for 2015 indicate a good level of accuracy, with an overall Kappa value of 0.69 and with a percentage of the correctness 76.28 %. ANN-Multi-layer perception model is then used to forecast changes in LULC for the years 2025 and 2030 which shows significant rise in cropland and built-up areas, by 20 $km^2$ and 10 $km^2$ respectively. The findings assist farmers and policymakers in developing optimal land use plans and better management techniques for the long-term development of natural resources.

**Keywords:** Land use and Land cover; ANN-Multi layer perception; Predicted LULC; Bhavani basin, MOLUSCE, QGIS

Manikandan Kamaraj
e-mail: mk6714@srmist.edu.in

1. Research Scholar, Department of Civil Engineering, College of Engineering and Technology, SRM Institute of Science and Technology, SRM Nagar,Kattankulathur, 603 203, Kanchipuram, Chennai, TN, India.

2. Associate Professor, Department of Civil Engineering, College of Engineering and Technology, SRM Institute of Science and Technology, SRM Nagar,Kattankulathur, 603 203, Kanchipuram, Chennai, TN, India.
e-mail: sathyanr5@srmist.edu.in

## Introduction

Biodiversity, distribution of water and radiation budgets, greenhouse gas emissions, carbon cycling, and livelihoods are all impacted by the land-use changes (LULC) around the world. The visual effect of land use at a given moment is known as land cover. Land use, on the other hand, refers to the amount of human activity that is directly tied to the land and the utilization of its resources (Ebenezer et al., 2018). LULC is gradually increased due to the following parameters interaction with climate, ecological processes, biogeochemical cycles, biodiversity, and human activities (Abdul Rahaman et al., 2017). LULC studies are generally adopted to know the change in ecology of the area and vegetation (El-Tantawi et al., 2019a). The change in LULC of a region, especially the increase in built-up areas, alters hydrological processes such as runoff pattern, peak flow characteristics, water quality, and so on (Ashaolu et al., 2019a). LULC, being considered one of the important factors of streamflow shift as it can alter the catchment's hydrological processes (Msovu et al., 2019). Humans have influenced and altered ground cover, either directly or indirectly (Buğday and Erkan Buğday, 2019). The role of the land, or the complete range of direct management activities that impact the

land's existence, such as agriculture, forestry, industry, and other associated activities, determines the land use. Land cover, on the other hand, refers to the current biophysical state of the earth's surface and immediate subsurface (Srivastava et al., 2020; Wang et al., 2021).Deforestation, desertification, soil erosion, and other forms of environmental destruction are all caused by the changes in land use and land cover (Bhattacharya et al., 2020). The combined remote sensing (RS) and geographical information system(GIS) has best tool for managing the land use change research and natural resources. Analyzing and tracking regional and temporal LULC shifts benefits scientists, environmentalists, agriculturalists, legislators, and urban planners. (Guidigan et al., 2019). Remote sensing techniques assist in the efficient preparation of natural resources, as well as land management and long-term change dynamics tracking (Ebenezer et al., 2018and Bhattacharya et al., 2020). LULC transition models, on the other hand, typically attempt to forecast when and how frequently these changes will occur. Land prediction models such as IDRISI's CA MARKOV, CLUE-S/ Dyna-CLUE, DYNAMICS EGO, and Land Change Modeler are being used by the researchers across the world. The future prediction model proved extremely helpful in determining how previous and future LULC changes may effect soil erosion, especially on farmland. (Perović et al., 2018). Several spatio-temporal prediction models, such as the Markov chain (MC) model, the Cellular Automata (CA) model, and the conversion of land use and its effects (CLUE) model, have been developed in recent years to forecast the LULC and their change detections (Alam et al., 2021a). Among this the CA model has been frequently used for land-use change analysis among the several spatio-temporal dynamic modeling approaches. MOLUSCE (Modules of Land Use Change Evaluation), a new QGIS plugin that can estimate potential LULC changes is built with CA model and also includes a transition probability matrix, is being used by most researchers (NEXTgis 2017). Four well-known algorithm models are employed in this plugin: Artificial Neural Networks (ANN), Logistic Regression (LR), Multi-criteria Evaluation (MCE), and Weights of Evidence (WoE). A CA-ANN model in MOLUSCE is a reliable tool for predicting future LULC that may be utilized in land use planning and management. This approach is being used for predicting the spatial LULC shift because it estimates the pixel's current condition based on its initial situation, adjacent neighbourhood eventuality, and changeover laws. Moreover this accurately depict nonlinear spatial stochastic LULC change processes and produce complex patterns (Saputra and Lee, 2019). CA models are also increasingly being used in urban planning studies. They are capable of replicating the spatiotemporal complexity of urban areas as well as deforestation caused by natural disasters or human actions (Saputra and Lee, 2019). MOLUSCE was developed to investigate a range of applications, including studying temporal LULC shifts and projecting future land use, anticipating prospective shifts in land cover and forest cover, and detecting deforestation in sensitive locations. (Aneesha Satya et al., 2020). This LULC change model, which is based on a multicriteria analysis methodology, was created using GIS software. (Mzava et al., 2019). To predict their relative effect on the model, the parameters depend on the researcher's response weight (Singh et al., 2014; Hassan et al., 2016). When dealing with human activities that may alter the region suited for biological populations temporally, the LULC has a significant impact on species distributions, which is one of the most essential environmental aspects to be considered. Using the ANN-Multi-Layer perception approach, this study on Bhavani river basin situated in Tamil Nadu, reveals to classify the changeover of land-use changes for the period 2005-2015, as well as to forecast and establish potential land-use changes in the years 2025 and 2030.

**Study Area**

The Bhavani river basin is located between latitudes 10º 56" 3' N to 11º 46" 14' N and longitude 76º 24" 41' E to 77º 41" 11' E in western Tamil Nadu, bordered on the north by the Upper Cauvery river basin aquifer system, on the south by the Amaravathy river basin aquifer system, on the east by the Lower Cauvery river aquifer system, and on the west by the Karnataka state (Wang et al., 2021). The Bhavani river rises in the Western Ghats' Nilgiri hills, flows through Kerala's Silent Valley National Park and returns to Tamil Nadu. The Bhavani is a 217 km long perennial river fed primarily by the southwest monsoon, with the northeast monsoon supplementing it. Its watershed covers 6,216 $km^2$; out of which nearly 87 % drains in Tamil Nadu, 9 % in Kerala, and 1 % in Karnataka. 90 % of Bhavani river water is used for irrigation and agriculture (Muthusamy et al., 2013; Narayanamurthi, 2020). The river flows

primarily through the Coimbatore and Erode districts in Tamil Nadu. The average annual rainfall of the Bhavani basin is 811.47 mm, ranging from 544.70 mm in Annur, Coimbatore district, to 2251.00 mm in Gudalore, Nilgiri district. The Bhavani basin drains 5537 $km^2$ in Tamil Nadu and is divided into three sections viz., Erode, Coimbatore, and Nilgiris (Muthusamy et al., 2013; Ministry of India water resources, 2017). In the previous 50 years, the population of the basin has increased by nearly 200 percent, to roughly 2.5 million people. More than half of the people in the Nilgiris district work in cattle, forestry, fishing, hunting, plantations, or orchards, and 14 % work as cultivators or harvesters. In the Erode district, agriculture employs about 55 % of the population, while non-agricultural activity employs the remaining 45 %. (Muthusamy et al., 2013). In this basin, most of the farmlands are irrigated either through canal or groundwater and remaining are rain fed with supplementary irrigation through groundwater (Muthusamy et al., 2013). Among the crops planted are sugarcane, paddy, peanuts, legumes, fodder sorghum, coconut, sesame, turmeric, and banana (Fig. 1).

**Data and Criteria**

The source of data set for the study includes digital elevation model (DEM), distance from road and river map and the three LULC thematic maps for the years 2005, 2010 and 2015. The LULC maps were obtained from the National Remote sensing Centre (NRC), Hyderabad, and the road maps were obtained from the open street map website (https://www.openstreetmap.org). The SRTM (Shuttle Radar Topography Mission) DEM was obtained from bhuvan Indian Geo-platform of ISRO. The detailed information of the source of data sets are given in Table 1.

The following parameters which were chosen for the study are DEM, slope map, aspect map, built-up land, and distance from the road map and river. In the LULC simulation and projection, the parameters were then divided into input data and descriptive data. The three thematic LULC maps include the initial input data, while the descriptive data includes DEM, gradient, aspect, distance from the road and river map, and built up density.

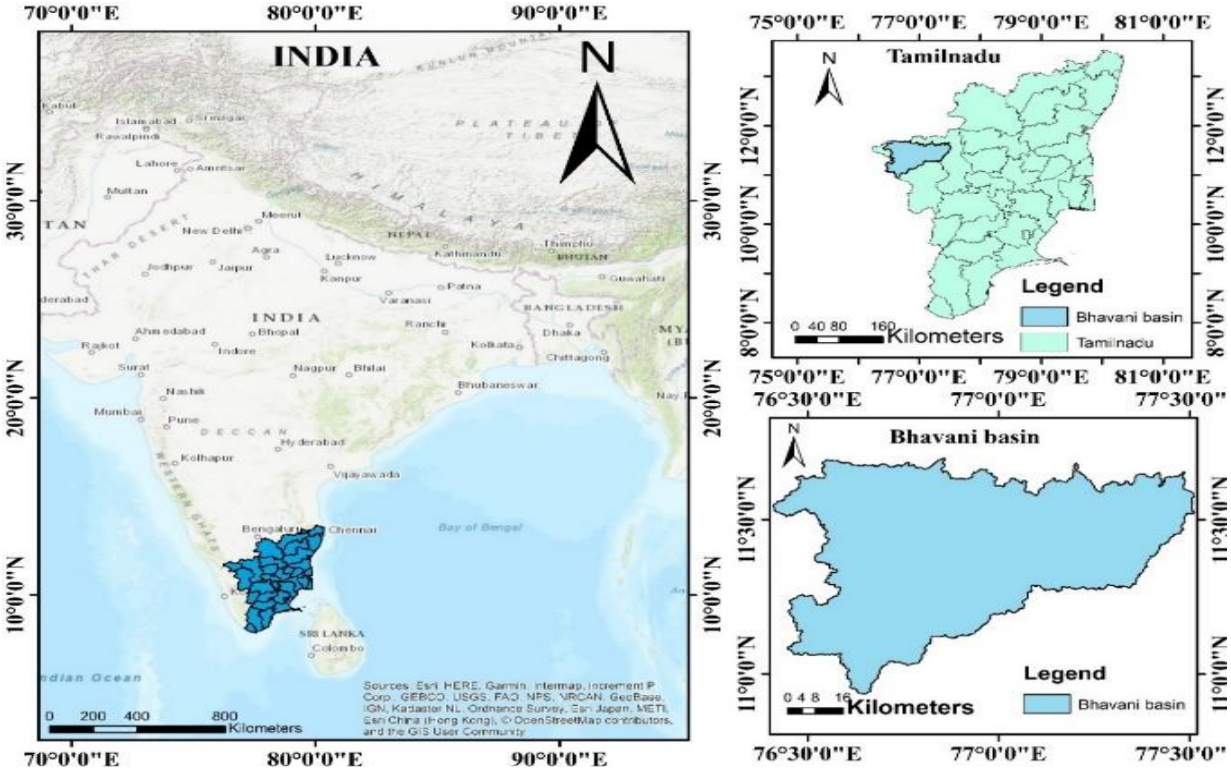


**Fig. 1** Location of the Bhavani basin

274 **Table 1** Source of Datasets maps

| Data | Criteria | LULC Simulation | Year | Description | Source | Data format |
|---|---|---|---|---|---|---|
| DEM | DEM Gradient Aspect | Special variable maps | 2019 | SRTM (Shuttle Radar Topography Mission with 30 m spatial resolution | National remote sensing Centre(NRSC) Bhuvan \| NRSC Open EO Data Archive \| NOEDA \| Ortho \| DEM \| Elevation \| AWiFS \| LISS III \| HySI \| TCHP \| OHC \| Free GIS Data \| Download | Tiff |
| Road &River map | Distance from the road | Special variable maps | 2017 | The main road map of Bhavani basin area | OpenStreetMap | .shp |
| LULC map | LULC | Input maps | 2005 2010 2015 | A satellite images from Landsat | National remote sensing Centre(NRSC) Welcome to Bhuvan \| ISRO's Geoportal \| Gateway to Indian Earth Observation (nrsc.gov.in) | .tif |

275
276
277 **Table 2** Eight categories of LULC maps

| | Classification | Description |
|---|---|---|
| 1 | Builtup Land | Buildings and other artificial structures occupy the land. |
| 2 | Crop Land | A brief farmed area is followed by harvest and a cycle of bare soil (e.g. single and multiple cropping systems). Perennial woody crops can be categorised as forest or shrubland depending on the environment. Orchards are included in the price. Seasons were not used to separate different forms of agriculture into divisions (e.g., Kharif, rabi, zaid). |
| 3 | Current fallow land | All arable land that is either part of a crop rotation system or is kept in good agricultural and environmental condition (GAEC), whether farmed or not, but will not be harvested for the duration of a crop year, is considered fallow land. |
| 4 | Plantations | Plantations, orchards, and tree cash crops for commercial horticulture |
| 5 | Forest | Deciduous forest, Evergreen forest, Scrubs forest. |
| 6 | Grassland | Herbaceous covers. Trees and shrubs cover less than 10 % of the area. |
| 7 | Wasteland | Land that is sparsely vegetated shows signs of erosion and land deformation due to lack of adequate water, soil management and natural causes. These are parcels of land that have been classified as underutilized and could be reclaimed for productive purposes with sufficient effort. Wasteland refers to a degraded forest with signs of deforestation (less than 10 % tree cover). |
| 8 | Water bodies | Surface water, whether impounded in ponds, lakes, or reservoirs, or flowing as streams, rivers and other bodies of water. Water bodies may be either fresh or salty. |

## Methods

In the Cellular Automation model, the transition probabilities from the ANN learning process are employed to describe the LULC changes. The (MOLUSCE) plugin in Quantum GIS 2.18.24 software is used for this method (Fig. 2). The MOLUSCE plugin features six LULC prediction phases (Hakim et al., 2019).

### 1. Inputs

This first step in the model is to include the LULC maps for the beginning (2005) and end year (2010). The spatial variable factors such as DEM, slope map, aspect map, distance from road and rivers, and built-up density are fed in the model to get a land cover change map from which the changing pattern for the study area between 2005 and 2010 is established (Fig.3). The properties of the explanatory maps are extracted in the same raster format for all datasets, with the same geographical projected coordinates of UTM 43N and with a resolution pixel size of 50 m.

The plugin calculates the percentage of area change in a given year and generates a transition matrix that shows the proportion of pixels shifting from one land use cover to another. The plugin also creates an area change map that shows the change in the land between 2005 and 2010 in all the eight classes' viz., built-up land, cropland, pasture, fallow land, forest, grassland, wasteland, and water bodies. To project the change in LULC, the ANN-(Multi layer perception) plugin was used (Buğday and Erkan Buğday, 2019; Msovu et al., 2019). Also, based on the classified raster images of 2005 and 2010, LULC transitions are predicted for the years 2025 and 2030. The future LULC maps are predicted assuming that existing LULC pattern and dynamics are getting continued.

### 2. Evaluation Correlation

The correlation of geographic variables between the two raster images, which are used to examine the correlation among the spatial variables factors, is evaluated using Pearson's correlation, Crammer's coefficient, and Joint information uncertainty. (Hakim et al., 2019). Then, between the initial year (2005) and the final year (2010), the category of each area and the LULC changes are calculated. The transition matrix, which indicates the fraction of pixels changing from one type to the next, is also produced by the algorithm.

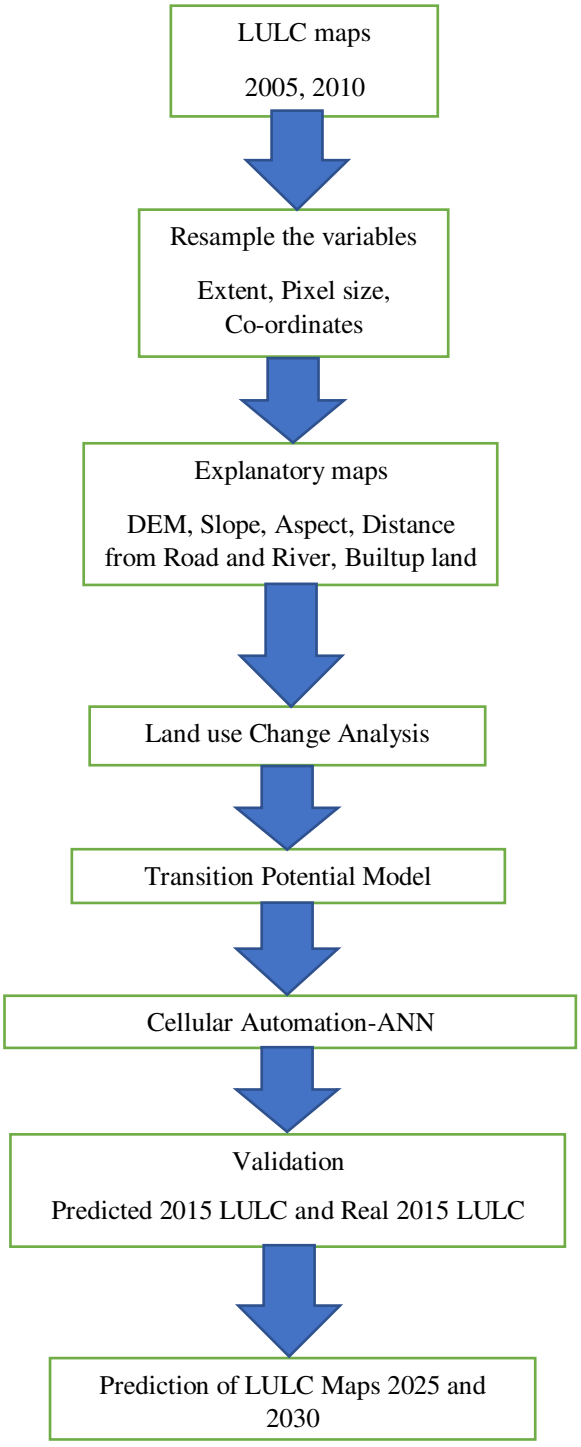


**Fig. 2** Flowchart of the methodology

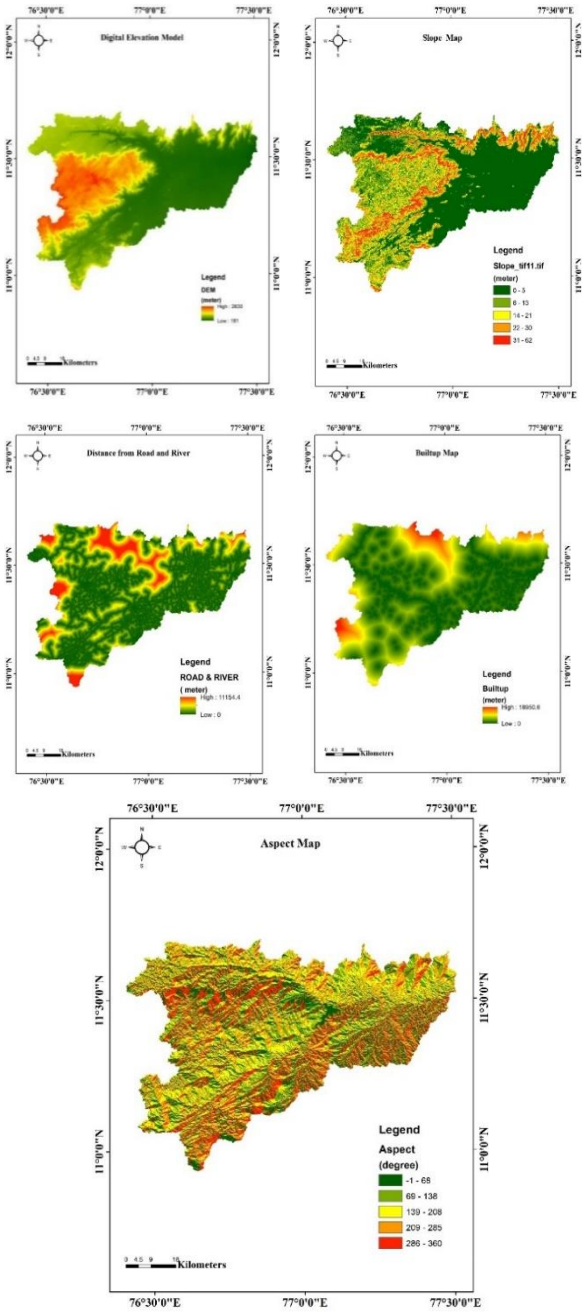


**Fig. 3.** Explanatory maps: DEM, Slope map, Distance from road and river, builtup density and Aspect map

## 3. Area Change

This stage calculates changes in area between the initial year (2005) and final year (2010) of the LULC. The changes in land use/cover area are represented in $km^2$. (Ashaolu et al., 2019b; Rahman et al., 2017b).

## 4. Transition Potential Modelling

While there are several methods for calculating transition potential maps, this plugin includes artificial neural networks (ANN), weights of evidence (WoE), logistic regression (LR), and Multi-Criteria Evaluation (MCE). For calibrating and modelling land use/cover changes, each methodology takes land use/cover change information and geographic factors as inputs. (Buğday and Erkan Buğday, 2019; El-Tantawi et al., 2019b; Guidigan et al., 2019). To model LULC forecast, the Artificial Neural Network (Multilayer Perception) technique was used for this study to forecast LULC map for the year 2015. The kappa coefficient was measured while validating the real and predicted LULC maps.

## 5. ANN-CA

While there are numerous ways for creating a transitional potential map, this module includes computational intelligence aspects such as artificial neural networks (ANN). LULC data is used as an input in every approach for calibrating and modelling LULC change. This strategy is justified in handling problems where the algorithm must deal with enormous amounts of uncertain or difficult-to-implement input data. As a result, a continuous index is created that describes the terrain on a scale of 0 to 1. Since ANN incorporates fuzzy logic requirements, a continuous range, such as 0 and 1, is determined based on terrain usability. The interactions between linked neurons and the alteration of the weight connections between them are the important elements of ANN (Bhattacharya et al., 2020). The following parameters were finally arrived while predicting the LULC map for the year 2015 viz., neighbourhood - 1, iterations – 1000 nos., hidden layer – 10 nos., momentum value - 0.06, learning rate - 0.001 (El-Tantawi et al., 2019c; Perović et al.,2018; Das and Sarkar, 2019) .

## 6. Validation

The assessment of LULC was measured widely by kappa coefficient. The validation is carried out between the predicted and real LULC maps of 2015 by calculating the overall kappa value. The Kappa coefficient is calculated using the expression given below (Ullah et al., 2019; Alawamy et al., 2020; Aneesha Satya et al., 2020)

$$kappa = \frac{po - pe}{1 - pe}$$

Where $p_o$ denotes the proportion of actual agreements and $p_e$ denotes the proportion of expected agreements.

$$po = \sum_{i=1}^{c} pij$$

$$pe = \sum_{i=1}^{c} piTpTj$$

Where $p_{ij}$ denotes the i-th and j-th cells in the contingency table, $p_iT$ denotes the sum of all cells in the i-th row, $pT_j$ denotes the sum of all cells in the j-th column, and c denotes the raster category count. The contingency table is a matrix that represents the frequency distribution of variables and is used in this study to show how the i-th and j-th cells are related. In a matrix, the interactions of each cell are tabulated and calculated. The result explains the agreement of every criterion of each cell (Saputra and Lee, 2019).

Several simulations were done to predict the LULC change map for 2015 utilising various combination of spatial variables factors, and for the analysis two to three spatial variables were combined to create an ANN-Multi layer perception (Table 3).

**Table 3.** Different combinations of explanatory maps and Kappa coefficients

| No | Spatial variable combinations | Percentage of kappa correctness | Kappa coefficients |
|---|---|---|---|
| 1 | DEM, Road, Built-up | 76.28 | 0.69 |
| 2 | DEM, Road | 73.12 | 0.60 |
| 3 | DEM, Built-up | 70.45 | 0.58 |
| 4 | DEM, Builtup, Urban, gradient | 71.01 | 0.56 |
| 5 | DEM, gradient, Aspect | 68.86 | 0.54 |

Table 3 discusses the overall accuracy and maximum kappa coefficients for the various spatial variable factors combinations. From the analysis it was found that the combinations of DEM, built-up density, distance from the road and river, got the maximum Kappa value of 0.69 and the maximum percentage of correctness 76.28 % (Fig.4). The maximum kappa value of 0.63 was considered as a good accuracy by many researchers (Alam et al., 2021b; Aneesha Satya et al., 2020; Perović et al., 2018; Rahman et al., 2017b). Hence it can be concluded that these variables have high influence on the predicted LULC map of this basin. The LULC map of 2025 and 2030 were predicted by using 2005 and 2010 LULC map along with the same spatial variable factors combinations.

## Results and Discussion

Table 4 displays the changeover probability matrix of LULC categories from 2005 to 2010. Except for the diagonal cells with high values, which show no changes because they remain in the same category, the value in the table ranges from 0 to 1, with higher values signifying bigger changes.

The trend of LULC change from 2005 to 2020 is summarised in Tables 5 and Table 6, which show the percentage of area covered under each LULC classes. (Fig.5) depicts the spatial variation of LULC from 2005 to 2020. In 2005, forest is dominated by 47.79 % of the total area, followed by cropland (16.65 %), plantation (15.50 %), fallow land (9.27%), wasteland (7.34 %), water bodies (2.03 %), built upland (1.40 %), and grassland (0.03 %). It was observed that except for water and grassland, changes in the trend were detected for all LULC between the years 2005, 2010, 2015, and 2020. When compared to 2005, the percentage of area covered in 2020 had decreased for forest land, fallow land, waste land and water bodies by 0.31 %, 3.28%, 1.67% and 0.02% respectively. An increase in percentage was observed for built-up land and crop land by 1.47% and 3.8% respectively. Change in area was not observed for the plantation and grassland category between the periods.

The change in land cover classes between 2015 and 2025 is depicted in Table 7.It is observed that the built-up and crop land will increase by 24.09 $km^2$ and 14.13 $km^2$, respectively, while fallow land, forest, and waste land will decline by 10.1 $km^2$, 11.79 $km^2$, and 16.14 $km^2$, respectively. Land use land cover changes as a percentage of total land area is also analysed. A positive value implies that the categorization has improved, while a negative value denotes the categorization has deteriorated.

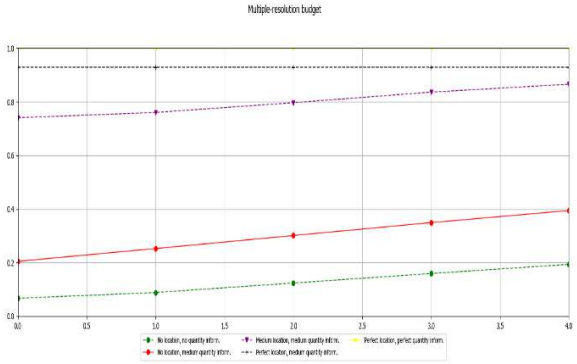


**Fig.4 Validation graph between observed 2015 and predicted 2015 LULC map**

513 **Table 4** Change over probability matrix LULC from 2005-2010

| | | 2010 | | | | | | | | |
|---|---|---|---|---|---|---|---|---|---|---|
| | Classification | Built-up Land | Crop Land | Fallow Land | Plantation | Forest | Grass Land | Waste Land | Water bodies | Sum |
| 2005 | Builtup Land | 0.979113 | 0.010186 | 0.006318 | 0.001418 | 0.00026 | 0 | 0.00065 | 0.00206 | 1 |
| | Crop Land | 0.001698 | 0.87721 | 0.10341 | 0.001471 | 0.00199 | 0 | 0.01345 | 0.00077 | 1 |
| | Fallow Land | 0.001398 | 0.439624 | 0.537976 | 0.001281 | 0.00155 | 0 | 0.01761 | 0.00056 | 1 |
| | Plantation | 0.000511 | 0.001696 | 0.00043 | 0.997213 | 0 | 0 | 9.3E-05 | 5.8E-05 | 1 |
| | Forest | 0.000053 | 0.000848 | 0.000128 | 0 | 0.99878 | 0 | 7.2E-05 | 0.00012 | 1 |
| | Grass Land | 0 | 0 | 0 | 0 | 0 | 1 | 0 | 0 | 1 |
| | Waste Land | 0.088227 | 0.076846 | 0.013515 | 0.001202 | 0.00113 | 0 | 0.81869 | 0.00039 | 1 |
| | Water bodies | 0.000621 | 0.009588 | 0.002219 | 0.000266 | 0.0008 | 0 | 0.00107 | 0.98544 | 1 |
| | Sum | 1.071621 | 1.415998 | 0.663996 | 1.002851 | 1.00451 | 1 | 0.85162 | 0.98941 | 8 |

514

515 **Table 5** LULC analysis from 2005-2020

| | 2005 | | 2010 | | 2015 | | 2020 | |
|---|---|---|---|---|---|---|---|---|
| LULC | Area in $km^2$ | % of area covered | Area in $km^2$ | % of area covered | Area in $km^2$ | % of area covered | Area in $km^2$ | % of area covered |
| Builtup Land | 77.56 | 1.40 | 114.85 | 2.07 | 141.48 | 2.55 | 159.68 | 2.87 |
| Crop Land | 924.67 | 16.65 | 1074.73 | 19.35 | 1125.21 | 20.25 | 1136.24 | 20.45 |
| Fallow Land | 515.19 | 9.27 | 379.78 | 6.84 | 340.48 | 6.13 | 332.57 | 5.99 |
| Plantation | 861.04 | 15.50 | 861.29 | 15.50 | 861.28 | 15.50 | 861.28 | 15.50 |
| Forest | 2654.74 | 47.79 | 2654.71 | 47.79 | 2644.89 | 47.61 | 2637.5 | 47.48 |
| Grass Land | 1.61 | 0.03 | 1.61 | 0.03 | 1.58 | 0.03 | 1.58 | 0.03 |
| Waste Land | 407.7 | 7.34 | 355.75 | 6.40 | 328.48 | 5.91 | 314.73 | 5.67 |
| Water bodies | 112.64 | 2.03 | 112.69 | 2.03 | 112.01 | 2.02 | 111.83 | 2.01 |

516

517

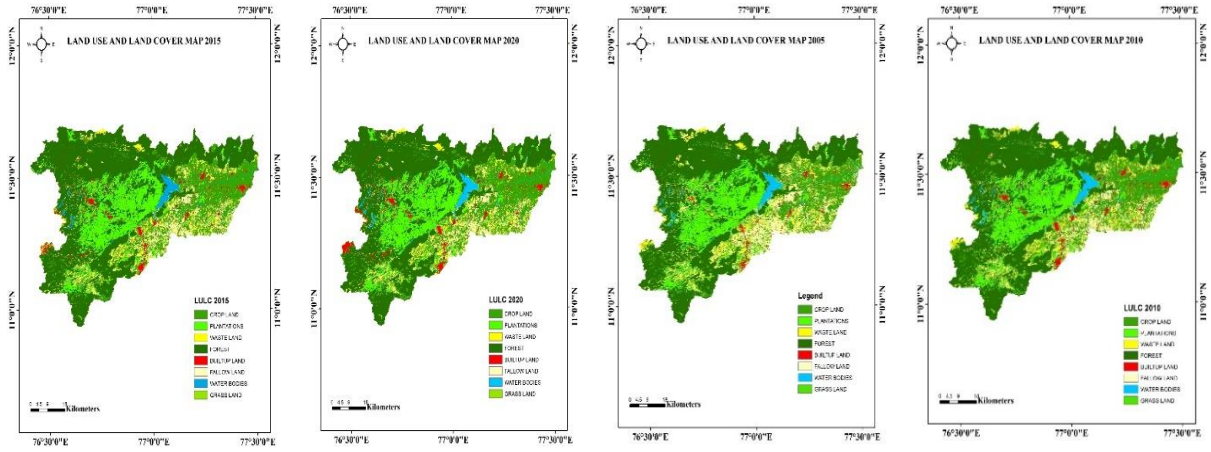


**Fig. 5** LULC maps for the year's 2005, 2010, 2015 and 2020

518

519

520 **Table 6** Land use land cover change analysis for every five years from 2005-2020

| YEAR | 2005-2010 | | 2010-2015 | | 2015-2020 | |
|---|---|---|---|---|---|---|
| | Area in km$^2$ | Changes % | Area in km$^2$ | Changes % | Area in km$^2$ | Changes % |
| Builtup Land | 37.29 | 0.671269 | 26.63 | 0.47935 | 18.2 | 0.327 |
| Crop Land | 149.86 | 2.697677 | 50.48 | 0.90866 | 11.03 | 0.198 |
| Fallow Land | -135.45 | -2.438278 | -39.3 | -0.7074 | -7.91 | -0.142 |
| Plantation | 0.25 | 0.0045 | -0.01 | -0.0002 | 0 | 0 |
| Forest | -0.03 | -0.00054 | -9.82 | -0.1768 | -7.39 | -0.133 |
| Grass Land | 0 | 0 | -0.03 | -0.0005 | 0 | 0 |
| Waste Land | -51.97 | -0.935528 | -27.27 | -0.4909 | -13.75 | -0.247 |
| Water bodies | 0.05 | 0.0009 | -0.68 | -0.0122 | -0.18 | -0.003 |

521

522

524

525 **Table 7** Distribution of LULC categories between 2015 and 2025

526

| | 2015 Year (km$^2$) | 2025 Year (km$^2$) | Change (km$^2$) | 2015% | 2025% | Δ % |
|---|---|---|---|---|---|---|
| Builtup Land | 141.48 | 165.57 | 24.09 | 2.55 | 2.98 | 0.434 |
| Crop Land | 1125.21 | 1139.34 | 14.13 | 20.25 | 20.51 | 0.254 |
| Fallow Land | 340.48 | 330.38 | -10.1 | 6.13 | 5.95 | -0.182 |
| Plantation | 861.28 | 861.28 | 0 | 15.50 | 15.50 | 0.000 |
| Forest | 2644.89 | 2633.1 | -11.79 | 47.61 | 47.40 | -0.212 |
| Grass Land | 1.58 | 1.58 | 0 | 0.03 | 0.03 | 0.000 |
| Waste Land | 328.48 | 312.34 | -16.14 | 5.91 | 5.62 | -0.291 |
| Water bodies | 112.01 | 111.82 | -0.19 | 2.02 | 2.01 | -0.003 |

527

528

529 .

530 **Table 8** Distribution of LULC categories between 2015 and 2030

| | 2015 Year (km$^2$) | 2030 Year (km$^2$) | Change (km$^2$) | 2015% | 2030% | Δ % |
|---|---|---|---|---|---|---|
| Built-up Land | 141.48 | 169.95 | 28.47 | 2.55 | 3.06 | 0.512 |
| Crop Land | 1125.21 | 1140.42 | 15.21 | 20.25 | 20.53 | 0.274 |
| Fallow Land | 340.48 | 329.64 | -10.84 | 6.13 | 5.93 | -0.195 |
| Plantation | 861.28 | 861.28 | 0 | 15.50 | 15.50 | 0.000 |
| Forest | 2644.89 | 2629.86 | -15.03 | 47.61 | 47.34 | -0.271 |
| Grass Land | 1.58 | 1.58 | 0 | 0.03 | 0.03 | 0.000 |
| Waste Land | 328.48 | 310.86 | -17.62 | 5.91 | 5.60 | -0.317 |
| Water bodies | 112.01 | 111.82 | -0.19 | 2.02 | 2.01 | -0.003 |

531

532

533

Table 8 shows how the land cover classifications have changed between 2015 and 2030. By 2030, an increase in area is observed for built-up areas and cropland by 28.47 km$^2$ and 15.21 km$^2$, respectively. For other categories except for plantation and grass land a decrease in area is forecasted. (Fig.6) shows the areal LULC changes of different categories from 2005 to 2030 in an incremental span of five years and (Fig.7) shows the expected land-use changes in 2025 and 2030.

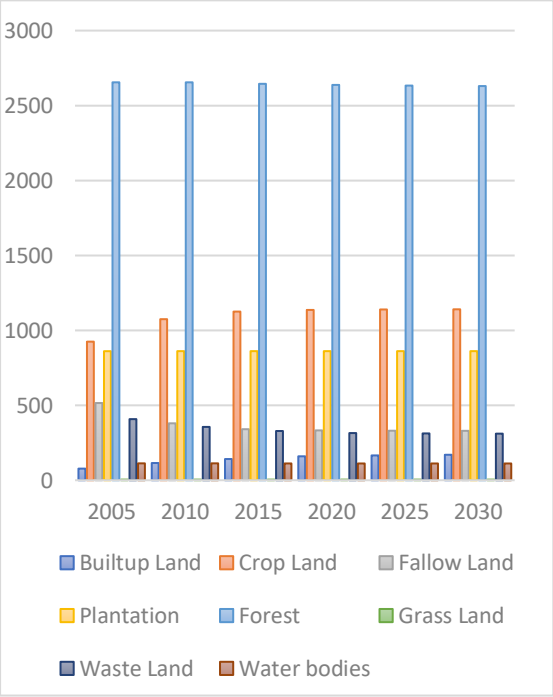


**Fig. 6** Change of LULC areas in km$^2$ from 2005 to 2030

The percentage difference in LULC categories from 2005 to 2025 and 2005 to 2030 showed an increase in built-up area and crop land by 1.58 %, and 3.86 %; 1.66 % and 3.88 % respectively, whereas for other categories a decrease in percentage (< 3%) was noticed. From the analysis it is learnt that when the area of one classification increases, it decreases the area of other classes and vice versa. Increase in cropland and built-up areas in the future imply that these categories have to be given importance in designing policy formulations for the basin.

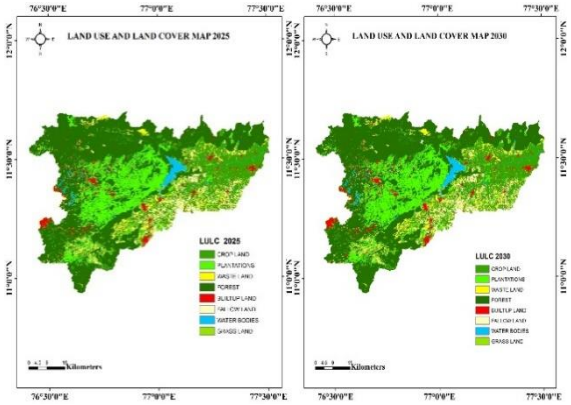


**Fig . 7** Predicted LULC maps for the year's 2025 and 2030

## Conclusion

The prediction of LULC plays a vital role in creating plans for balancing conservation, competing users, and developmental pressures. The ANN-Cellular Automation model is utilized to simulate and predict the future LULC maps of the Bhavani basin, Tamil Nadu. The three spatial variable factors viz., DEM, distance from the road and river, and built-up density, had a huge effect to predict LULC map of this basin. The Kappa value of 0.69 shows a maximum level of accuracy between the observed and predicted 2015 LULC maps. The LULC map of 2025 and 2030 were predicted by using 2005 and 2010 LULC map along with same spatial variable factors combinations. The predicted LULC for the years 2025 and 2030 show significant increase in cropland and built-up areas by 20 km$^2$ and 10 km$^2$ respectively. Meanwhile, relative to the year 2015 LULC, fallow land, forest land, and wasteland areas are expected to decrease by 10 km$^2$, 11 km$^2$, 16 km$^2$ by 2025, and 10 km$^2$,15 km$^2$ and 17 km$^2$ by 2030. The results demonstrate that due to anthropogenic pressures the conversion of forest land and other land categories would be converted to builtup land and crop land areas.

The forest region in the Nilgiri hills of the Western ghats is a key forest area in Tamil Nadu, which needs significant preservation and conservation. Forest disturbance, particularly land conversion, does, nevertheless, result in forest degradation. Rather than being retained as forest, human interests in the region drive the land to be transformed to extra creative uses, such as farmland or industrial types. Conflicts over land interests in general, results in LULC modifications. Residents, for example, prefer crop plantings for reforestation, whereas businesses extend their plantations to boost earnings, reducing the region's wooded land. This situation necessitates a LULC approach that emphasizes the change's long-

term consequences, notably forest biodiversity loss. This study assists us in detecting specific land-use changes and projecting which land uses will be affected by future changes. It is also possible to detect biodiversity loss and ecological concerns. The findings assist farmers and policymakers in developing optimal land use planning and management methods for the long-term development of natural resources.

**Author contribution**

MK carried out all technical details and prepared the map and performed GIS analysis. SR contributed to the verification of the analysis and the results. MK has written the manuscript in consultation with SR. Both authors contributed to shape the work by discussing the results and contributed to the final manuscript.

**Funding:** Not applicable

**Availability of data and materials:**

The Land use and Land cover (LULC) maps used for the current study are obtained from the National Remote sensing Centre (NRC), Hyderabad, (https://bhuvan.nrsc.gov.in/bhuvan_links.php) and the road maps are obtained from the open street map (https://www.openstreetmap.org). The SRTM (Shuttle Radar Topography Mission) DEM for this study is obtained from bhuvan Indian Geo-platform of ISRO (https://bhuvan-app3.nrsc.gov.in/data/download/index.php).

**Declarations**

**Ethical approval:** Not applicable

**Consent to participate:** Not applicable

**Consent to publish:** Not applicable

**Competing interests:** The authors declare that they have no competing interests.

**References**

Abdul Rahaman, S., Aruchamy, S., Balasubramani, K., Jegankumar, R., 2017. Land use/land cover changes in a semi-arid mountain landscape in Southern India: A geoinformatics based Markov chain approach. International Archives of the Photogrammetry, Remote Sensing and Spatial Information Sciences - ISPRS Archives 42, 231–237. https://doi.org/10.5194/isprs-archives-XLII-1-W1-231-2017

Alam, N., Saha, S., Gupta, S., Chakraborty, S., 2021a. Prediction modeling of riverine landscape dynamics in the context of sustainable management of floodplain: a Geospatial approach. Annals of GIS. https://doi.org/10.1080/19475683.2020.1870558

Alam, N., Saha, S., Gupta, S., Chakraborty, S., 2021b. Prediction modeling of riverine landscape dynamics in the context of sustainable management of floodplain: a Geospatial approach. Annals of GIS. https://doi.org/10.1080/19475683.2020.1870558

Alawamy, J.S., Balasundram, S.K., Hanif, A.H.M., Sung, C.T.B., 2020. Detecting and analyzing land use and land cover changes in the Region of Al-Jabal Al-Akhdar, Libya using time-series Landsat data from 1985 to 2017. Sustainability (Switzerland) 12. https://doi.org/10.3390/su12114490

Aneesha Satya, B., Shashi, M., Deva, P., 2020. Future land uses land cover scenario simulation using open source GIS for the city of Warangal, Telangana, India. Applied Geomatics 12, 281–290. https://doi.org/10.1007/s12518-020-00298-4

Ashaolu, E.D., Olorunfemi, J.F., Ifabiyi, I.P., 2019a. Assessing the Spatio-Temporal Pattern of Land Use and Land Cover Changes in Osun Drainage Basin, Nigeria. Journal of Environmental Geography 12, 41–50. https://doi.org/10.2478/jengeo-2019-0005

Ashaolu, E.D., Olorunfemi, J.F., Ifabiyi, I.P., 2019b. Assessing the Spatio-Temporal Pattern of Land Use and Land Cover Changes in Osun Drainage Basin, Nigeria. Journal of Environmental Geography 12, 41–50. https://doi.org/10.2478/jengeo-2019-0005

Bhattacharya, R.K., das Chatterjee, N., Das, K., 2020. Land use and Land cover change and its resultant erosion susceptible level: an appraisal using RUSLE and Logistic Regression in a tropical plateau basin of West Bengal, India, Environment, Development, and Sustainability. Springer Netherlands. https://doi.org/10.1007/s10668-020-00628-x

Buğday, E., Erkan Buğday, S., 2019. Modeling and simulating land use/cover change using the artificial neural network from remote sensing data. Cerne 25, 246–254. https://doi.org/10.1590/01047760201925022634

Das, S., Sarkar, R., 2019. Predicting the land use and land cover change using Markov model: A catchment level analysis of the Bhagirathi-Hugli River. Spatial Information Research 27, 439–452. https://doi.org/10.1007/s41324-019-00251-7

Ebenezer, B., Geophery, K.A., Jonathan, A.Q.-B., Emmanuel, A.D., 2018. Land-use change and sediment yield studies in Ghana: Review. Journal of Geography and Regional Planning 11, 122–133. https://doi.org/10.5897/jgrp2018.0707

El-Tantawi, A.M., Bao, A., Chang, C., Liu, Y., 2019a. Monitoring and predicting land use/cover changes in the Aksu-Tarim River Basin, Xinjiang-China (1990–2030). Environmental Monitoring and Assessment 191, 1–18. https://doi.org/10.1007/s10661-019-7478-0

El-Tantawi, A.M., Bao, A., Chang, C., Liu, Y., 2019b. Monitoring and predicting land use/cover changes in the Aksu-Tarim River Basin, Xinjiang-China (1990–2030). Environmental Monitoring and Assessment 191. https://doi.org/10.1007/s10661-019-7478-0

El-Tantawi, A.M., Bao, A., Chang, C., Liu, Y., 2019c. Monitoring and predicting land use/cover changes in the Aksu-Tarim River Basin, Xinjiang-China (1990–2030). Environmental Monitoring and Assessment 191. https://doi.org/10.1007/s10661-019-7478-0

Guiding an M.L.G., Sanou, C.L., Ragatoa, D.S., Fafa, C.O., Mishra, V.N., 2019. Assessing Land Use/Land Cover Dynamic and Its Impact in Benin Republic Using Land Change Model and CCI-LC Products. Earth Systems and Environment 3, 127–137. https://doi.org/10.1007/s41748-018-0083-5

Hakim, A.M.Y., Baja, S., Rampisela, D.A., Arif, S., 2019. Spatial dynamic prediction of land use / landcover change (case study: Tamalanrea sub-district, makassar city), in: IOP Conference Series: Earth and Environmental Science. Institute of Physics Publishing. https://doi.org/10.1088/1755-1315/280/1/012023

Hassan, Z., Shabbir, R., Ahmad, S.S., Malik, A.H., Aziz, N., Butt, A., Erum, S., 2016. Dynamics of land use and land cover change (LULCC) using geospatial techniques: a case study of Islamabad Pakistan. SpringerPlus 5. https://doi.org/10.1186/s40064-016-2414-z

Ministriy of India water resources, 2017. Central Ground Water Board Ministry of Water Resources, River Development and Ganga Rejuvenation Government of India AQUIFER MAPPING AND GROUNDWATER.

Msovu, U.E., Mulungu, D.M., Nobert, J.K., Mahoo, H., 2019. Land Use/Cover Change and their Impacts on Streamflow in Kikuletwa Catchment of Pangani River Basin, Tanzania, Tanzania Journal of Engineering and Technology (Tanz. J. Engrg. Technol.).

Muthusamy, S., Krishnamurthy, R.R., Jayaprakash, M., Mohana Perumal, P., 2013. Geo-Environmental Analysis Using Multitemporal Satellite Data and GIS Techniques-A Case Study for Bhavani River Basin, Tamil Nadu, India, Cloud Publications International Journal of Advanced Remote Sensing and GIS.

Mzava, P., Nobert, J., Valimba, P., 2019. Land Cover Change Detection in the Urban Catchments of Dar es Salaam, Tanzania using Remote Sensing and GIS Techniques. Tanzania Journal of Science 45, 315–329.

Narayanamurthi, V., 2020. Impact of climate change in sediment yield from the catchment of Bhavani Sagar reservoir using SWAT model.

NextGIS. (2017). "MOLUSCE-quick and Convenient Analysis of LandCoverChanges." https://nextgis.com/blog/molusce/ (accessed 01 May 2019).

Perović, V., Jakšić, D., Jaramaz, D., Koković, N., Čakmak, D., Mitrović, M., Pavlović, P., 2018. Spatio-temporal analysis of land use/land cover change and its effects on soil erosion (Case study in the Oplenac wine-producing area, Serbia). Environmental Monitoring and Assessment 190. https://doi.org/10.1007/s10661-018-7025-4

Rahman, M.T.U., Tabassum, F., Rasheduzzaman, M., Saba, H., Sarkar, L., Ferdous, J., Uddin, S.Z., Zahedul Islam, A.Z.M., 2017a. Temporal dynamics of land use/land cover change and its prediction using CA-ANN model for southwestern coastal Bangladesh. Environmental Monitoring and Assessment 189. https://doi.org/10.1007/s10661-017-6272-0

Rahman, M.T.U., Tabassum, F., Rasheduzzaman, M., Saba, H., Sarkar, L., Ferdous, J., Uddin, S.Z., Zahedul Islam, A.Z.M., 2017b. Temporal dynamics of land use/land cover change and its prediction using CA-ANN model for southwestern coastal Bangladesh. Environmental Monitoring and Assessment 189. https://doi.org/10.1007/s10661-017-6272-0

Saputra, M.H., Lee, H.S., 2019. Prediction of land use and land cover changes for North Sumatra, Indonesia, using an artificial-neural-network-based cellular automaton. Sustainability (Switzerland) 11. https://doi.org/10.3390/su11113024

Singh, P., Gupta, A., Singh, M., 2014. Hydrological inferences from watershed analysis for water resource management using remote sensing and GIS techniques. Egyptian Journal of Remote Sensing and Space Science 17, 111–121. https://doi.org/10.1016/j.ejrs.2014.09.003

Srivastava, R., Singh, S., Oran, A., 2020. Changes in Vegetation Cover Using GIS and Remote Sensing: A Case Study of South Campus BHU, Mirzapur, India. Journal of scientific research 64, 135–141. https://doi.org/10.37398/jsr.2020.640219

Ullah, S., Tahir, A.A., Akbar, T.A., Hassan, Q.K., Dewan, A., Khan, A.J., Khan, M., 2019. Remote sensing-based quantification of the relationships

between land use land cover changes and surface temperature over the lower Himalayan region. Sustainability (Switzerland) 11. https://doi.org/10.3390/su11195492

Wang, S.W., Munkhnasan, L., Lee, W.-K., 2021. Land use and land cover change detection and prediction in Bhutan's high altitude city of Thimphu, using cellular automata and Markov chain. Environmental Challenges 2, 100017. https://doi.org/10.1016/j.envc.2020.1000

840